Proceedings of the 2020 Design of Medical Devices Conference
DMD2020
April 6, 7-9, 2020, Minneapolis, MN, USA

DMD2020-9061

A HYDRAULIC BIMODAL ANKLE TO IMPROVE MOBILITY AND STABILITY FOR PROSTHESIS USERS

Sara Koehler-McNicholas[1]
Minneapolis VA Health Care System
University of Minnesota
Minneapolis, MN, USA

Gregory Voss
Minneapolis VA Health Care System
Minneapolis, MN, USA

Evandro Ficanha
WillowWood
Mt. Sterling, OH, USA

John Looft
Minneapolis VA Health Care System
Minneapolis, MN, USA

Nicole Walker
Minneapolis VA Health Care System
Minneapolis, MN, USA

James Colvin
WillowWood
Mt. Sterling, OH, USA

Andrew Hansen
Minneapolis VA Health Care System
University of Minnesota
Minneapolis, MN, USA

Matthew Wernke
WillowWood
Mt. Sterling, OH, USA

ABSTRACT

A bimodal prosthetic ankle-foot system has been developed to support the demands of both walking mobility and standing balance. Using a novel hydraulic locking mechanism, this system provides a curved effective rocker shape for walking and a flat effective rocker shape for standing and swaying on non-level surfaces. To date, the hydraulic cylinder sub-assembly has been cycle tested to 1.2 million cycles. Future testing with lower-limb prosthesis users is planned, which will reveal the extent to which this new hydraulic ankle-foot design improves standing balance on both level and non-level surfaces. The capacity for an automatic switching algorithm, designed to appropriately detect and switch between modes as users transition between walking and standing tasks, will also be evaluated.

[1]Contact author: sara.koehler@va.gov

1.0 INTRODUCTION

The human ankle-foot system is a complex joint that plays an essential role in balance control during common activities of daily living (e.g., standing, swaying, and walking) by conforming to two simple yet distinctly different effective rocker shapes. Previous studies have shown that during walking, the ankle-foot system conforms to a curved effective rocker shape, which remains consistent for different walking speeds [1], for added weight carried on the trunk [2], and for shoes of different heel heights [3] and rocker profiles [4]. The radius of this curved shape, equal to approximately one-third of the total leg length, creates an inherently unbalanced system, supporting the common description of walking as "falling from one foot to the other." By contrast, the effective rocker shape formed by the same ankle-foot system is much flatter during standing and swaying, resulting in a rocker radius that is approximately twice that of the total leg length (i.e., six times larger than the rocker radius of walking). Accordingly, the human ankle-foot system conforms to an inherently stable effective rocker shape during standing and swaying, providing a nearly flat base of support for these tasks.

Following amputation, individuals who use a lower-limb prosthesis must learn to balance by relying on their intact limb, postural control strategies that have been altered by reduced sensation and muscle strength on their affected limb, and the mechanical properties of their prosthesis. Ideally, prosthetic ankle-foot systems should mimic the function of the anatomical joint by providing a flat effective rocker shape for standing and swaying [5]. However, most commercially-available ankle-foot prostheses are designed with a curved effective rocker shape for walking [6]. As a result, many individuals who use an ankle-foot prosthesis experience reduced balance and balance confidence while standing, which has been shown to negatively impact participation in social activities and quality of life [7-9].

To address the demands of both standing and walking, our group has designed a novel bimodal ankle-foot prosthesis [6,10] that can accommodate both functional modes through the use of a rigid footplate and an ankle that can lock (resulting in a flat effective rocker shape for standing) and unlock (resulting in a curved effective rocker shape for walking). In our first-generation prototype, switching between these two modes was achieved by changing the position of a slider mechanism, driven by a linear actuator (Fig 1). During clinical testing of this prototype, our group found that in the absence of visual feedback, the locked bimodal ankle improved static balance in a group of experienced, relatively active lower-limb prosthesis users (n=18) standing on a level surface [6]. Subjective feedback indicated that all subjects felt either equally balanced or more balanced when the ankle was locked compared to when it was unlocked, and 14 subjects expressed interest in trying the system for a longer period of time.

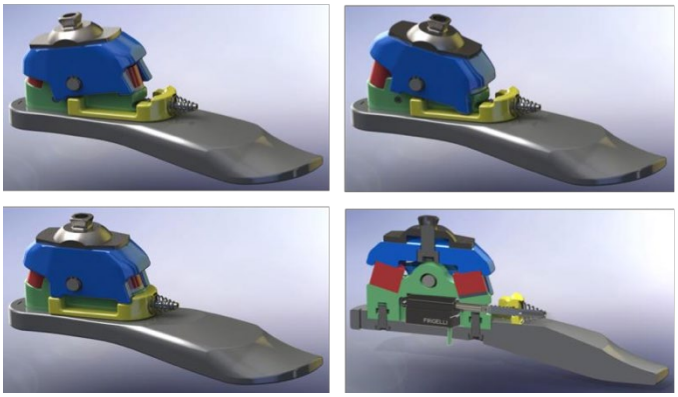

Figure 1. The bimodal ankle-foot system shown in the walking mode (top) and standing mode (lower left). The system uses a linear actuator (lower right) to push a slider mechanism (shown in yellow).

Subjective feedback obtained during this clinical testing also uncovered a new customer requirement: an ankle-foot system that could provide a stable base of support during standing and swaying tasks on *non-level* surfaces. This paper describes how this new customer requirement was decomposed into design specifications for a second-generation prototype of the bimodal ankle-foot system and how the design of this system has evolved to fulfill the goal of an ankle capable of continuous locking angles for non-level surfaces.

2.0 DEFINITION OF DESIGN SPECIFICATIONS

To provide a stable base of support on non-level standing surfaces, the design specifications of the first-generation bimodal ankle-foot prototype were reviewed and revised. The following design specifications were developed based on key parameters of standing and walking:

1. In the unlocked mode, the friction force from the unactuated locking system should be less than 5% of the peak ankle torque during walking.
2. The locking position should be continuously selectable from -12 degrees to +12 degrees relative to the neutral position.
3. In the locked mode, the ankle position should remain within 0.25 degrees of the locked position while under load from a 150 kg person for 24 hours.

Based on an analysis of these design specifications, hydraulic actuation was selected as the preferred design implementation. The primary drivers for selecting hydraulic technology were: 1) resistance to dirt and debris that would cause failure of the mechanism, 2) the ability to lock the ankle at any angle, rather than having to select from a discrete number of locking angles, 3) an updated look that progresses this concept past the appearance of the single-axis foot that was introduced over 20 years ago, and 4) a more robust design due to the reduction of parts that could ultimately fatigue and fail over time.

3.0 IDENTIFICATION OF HIGH-RISK TECHNICAL ASPECTS

Given the dependence of Design Specifications 1 and 3 on cylinder function, as well as our limited design experience with this branch of hydraulics technology, we identified the design of the hydraulic cylinder as the greatest technical risk. To mitigate this risk, a preparatory project was undertaken to generate evidence that the proposed hydraulic approach was technically viable.

A series of easy-to-assemble hydraulic cylinders were designed and constructed to test a range of seal designs and cylinder diameters against the two competing design specifications of low damping (Design Specification 1) and low ankle-angle drift (Design Specification 3). From Design Specification 1, the friction force within the cylinder needed to be less than 71 N, which was based on ISO mechanical testing standards for a P3 user (the lightest target user). From Design Specification 3, drift in the locked position needed to be less than 0.25 degrees, which translated to a cylinder drift of 2.3 mm. The cylinders were tested in both the locked and unlocked configuration in a universal test machine (Fig 2). Friction force in the cylinder was between 35 N and 59 N, at frequencies of 4 Hz and 0.5 Hz, respectively, which met the specification of less than 71 N. Drift in the locked position was 1.2 mm, which met

the specification of less than 2.3 mm. These results confirmed that using a hydraulic cylinder could deliver the performance required in the re-designed ankle-foot system.

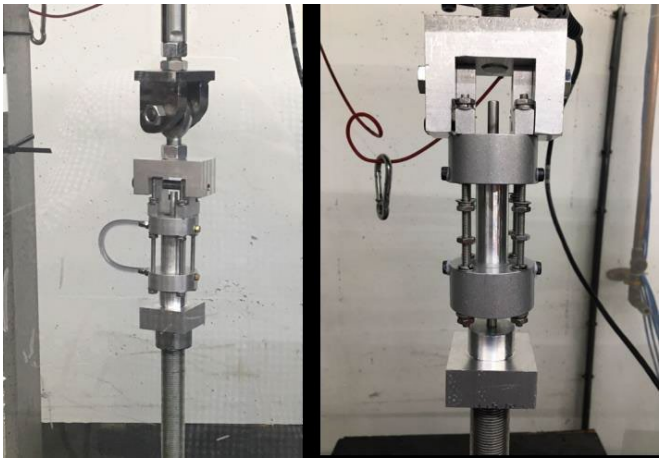

Figure 2. Cylinder testing for unlocked friction force (left) and locked drift (right).

4.0 DESIGN AND MECHANICAL TESTING OF THE HYDRAULIC CYLINDER

Several design iterations resulted in the final hydraulic cylinder design shown in cross section in Fig 3. The cylinder is 15.9 mm in diameter and allows 19.1 mm of travel and can lock in position under full toe loading without leakage. The piston and cylinder are constructed from T-303SS. The sealing elements (shown in green) are quad rings for the sliding surfaces to reduce compression force, and thereby friction, while maintaining adequate squeeze to maintain seal integrity. The endcaps (shown in purple) are constructed from 7075-T6 aluminum and are both floating, allowing the linear bearings (shown in orange) to maintain alignment and prevent binding without requiring precise machining. To reduce viscous damping, caused by friction in flowing hydraulic fluid, and reduce overall system size, the flow channel between the two chambers of the cylinder is machined into the piston rod. The valving mechanism itself is machined into the posterior end of the piston rod to prevent exposure to mechanical loading that is applied to the anterior end of the rod. As a result, the posterior end of the rod can be hollowed out without compromising structural integrity.

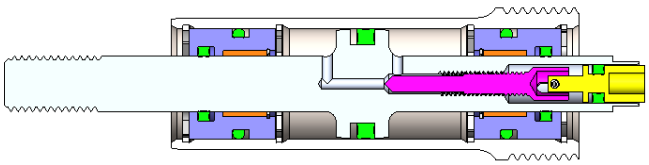

Figure 3. Final cylinder cross section.

Cylinder locking and unlocking is performed by an internal valve (shown in pink and yellow). The valve stem (shown in pink) uses a simple screw mechanism to translate between the locked and unlocked position. The valve drive link (shown in yellow) provides a sliding interface on one end to the valve stem and a fixed interface to the driving motor (not shown). Locking can be obtained in 250 msec (or 0.7 rotations). To date, the cylinder sub-assembly has been cycle tested to 1.2 million cycles.

5.0 ITERATIVE DESIGN OF THE BIMODAL ANKLE-FOOT SYSTEM

With the primary risk element of the design mitigated, several design iterations of the bimodal ankle-foot system were generated in order to integrate the cylinder control mechanism. The design started from a stripped-down kinematic model (Fig 4) to determine acceptable cylinder locations based on volume constraints and piston travel required to get acceptable ankle rotation.

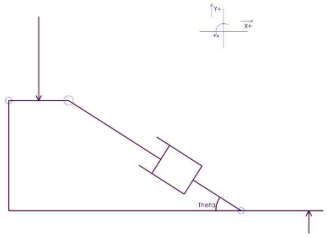

Figure 4. Kinematic model of ankle-foot system.

Based on this initial kinematic model, the hydraulic cylinder was placed in the forefoot in a primarily vertical orientation. Two different methods for allowing ankle rotation were explored: a dual "C" spring model (Fig 5) and a single-axis model (Fig 6). The dual "C" spring model was eliminated, since achieving the required ankle rotation required strains that were not obtainable within the volume constraints of a foot shell.

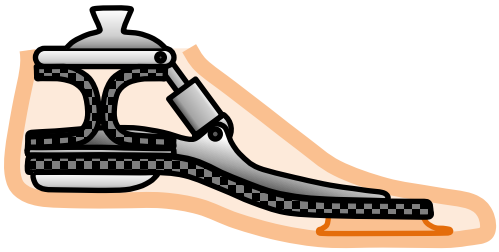

Figure 5. Dual "C" spring model with cylinder.

To simplify the design, the initial single-axis model (Fig 6) was constructed without resistive elements to control ankle actuation during walking. In single-axis ankle-foot designs, elastomeric bumpers are often used to generated ankle torque in response to ankle rotation and provide a smooth walking actuation. These elastomeric bumpers are generally oriented vertically with one bumper positioned anterior to the ankle axis to control dorsiflexion during forefoot loading and one bumper positioned posterior to the ankle axis to control plantarflexion during heel loading.

Figure 6. Single-axis implementation with cylinder.

Using a traditional bumper orientation was not possible within the volume constraints of a prosthetic foot shell. Additionally, placing the hydraulic cylinder horizontally next to the bottom of the foot surface utilized otherwise unusable space in the foot shell while releasing a claim on space in the ankle section of the foot.

To accommodate the horizonal orientation of the hydraulic control cylinder (Fig 7, shown in green), the ankle axis was relocated proximal and posterior in the foot. The anterior dorsiflexion bumper (shown in orange) remained in a vertical orientation, but the posterior plantarflexion bumper (shown in pink) was positioned in a horizonal orientation, with the connection of the control cylinder to the ankle attachment (shown in charcoal) located at the base of the foot. Although the two elastomeric bumpers appear to intersect, this is not the case. The pink plantarflexion control bumper is in fact two bumpers, one located on each side of the orange dorsiflexion bumper. Dividing the plantarflexion control into two bumpers resulted in a slender beam that buckled rather than compressed during testing.

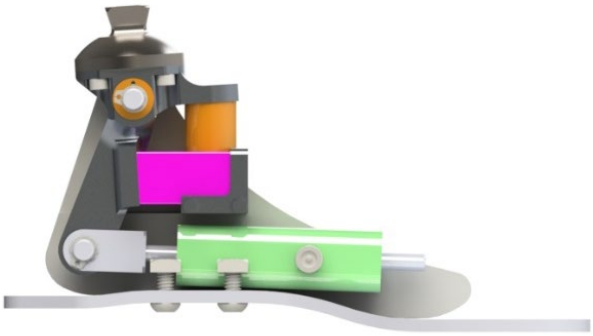

Figure 7. Single-axis design with horizontal cylinder.

To eliminate buckling, one final design change was implemented (Fig 8). The plantarflexion bumper (shown in pink) was tilted and relocated relative to the dorsiflexion bumper (shown in orange). Relocating the bumper allowed for the creation of a larger cross section and for the ankle actuation mechanism (shown in gray) to wrap around and support the plantarflexion bumper, preventing buckling.

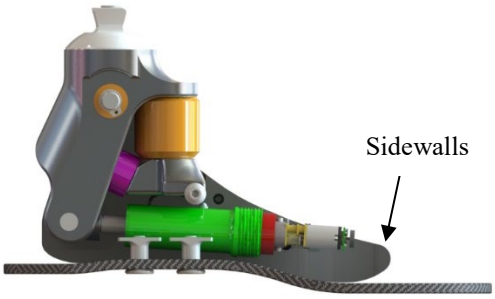

Figure 8. Single-axis design with horizontal cylinder and optimized bumper location.

6.0 HUMAN SUBJECT TESTING OF THE BUMPERS, SIDEWALLS, AND FOOTPLATE

With the locations of the hydraulic cylinder and bumpers optimized, it was important to verify the extent to which the bimodal ankle design provided a biomimetic rocker shape for walking and standing. As shown in Fig 8, the rocker profile of the foot is significantly influenced by the degree of overlap between the rigid and flexible materials of the foot assembly. The rigid sidewalls provide stiffness for a flat effective rocker shape when the ankle is locked, while the bumpers and flexible carbon footplate (i.e., the portion that extends beyond the sidewalls) allow for a curved rocker shape when the ankle is unlocked. To evaluate the roll-over shape (ROS) characteristics of the bimodal ankle-foot system during standing, swaying, and walking, motion analysis data were collected on a single lower-limb prosthesis user (height=1.85 m) using a modified version of the prototype shown in Fig 8. Instead of a hydraulic locking mechanism, a mechanical locking mechanism was used to manually lock and unlock the ankle.

Bumpers were selected based on the preference of the user. Several bumper combinations were evaluated by the subject until he felt like the transition between the heel and toe while walking was smooth. The same process was used to select the footplate. In order to minimize the effect of foot shell and shoe compression on the ROS characteristics of the foot assembly, the bimodal ankle was tested without a foot shell or shoe. Instead, a rigid crepe layer was built onto the plantar surface of the footplate with a 3/8'' heel lift and an overall height to prevent a leg length discrepancy. A certified prosthetist aligned the bimodal ankle-foot prosthesis, which was connected to the subject's usual prosthetic socket.

Roll-over shape data were collected using an 8-camera motion capture system (Oqus-7, Qualisys Motion Capture Systems, Gothenburg, Sweden) and a single force plate (AMTI, Watertown, MA, USA). The method used to measure and characterize the ROS of the bimodal ankle has been described previously [11]. A modified Helen Hayes marker set was used for data collection, with reflective markers placed on the sidewalls of the foot assembly to define the foot segment. Starting with the ankle unlocked, the subject was instructed to walk at his normal walking speed until three clean force plate

strikes were collected. The bimodal ankle was then locked, and the subject was instructed to stand with his prosthetic foot on the force plate while 8 sec of standing and 30 sec of swaying data were collected.

Fig 9 shows the mean ROS profile of the bimodal ankle measured during walking, swaying, and standing. It is apparent that during swaying, the locked bimodal ankle provided a much flatter rocker shape than the unlocked ankle during walking. The radius of these shapes is shown in Fig 10. During walking, the mean ROS radius was 56±4% of the subject's total leg length. For comparison, the mean ROS radius of the anatomical ankle-foot mechanism during walking is approximately 33%. During swaying, the ROS radius of the bimodal ankle was 256% of the total leg length, well over the 200% target observed for the unimpaired ankle-foot system.

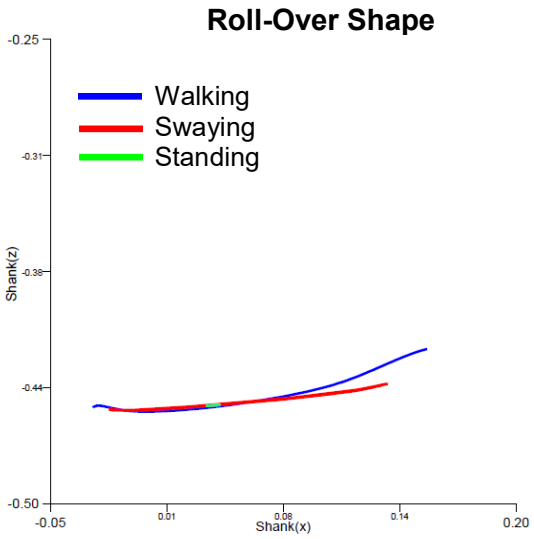

Figure 9. Roll-over shape profiles for walking, swaying and standing.

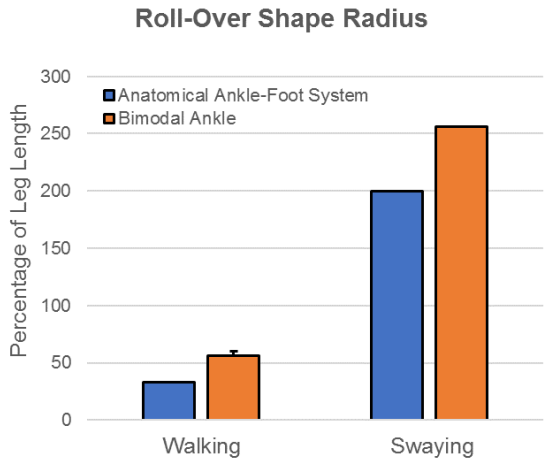

Figure 10. Roll-over shape radius measured during walking and swaying with the bimodal ankle.

Fig 11 shows that during the subject's normal walking speed, the stance-phase range-of-motion (ROM) of the bimodal ankle was approximately 18±1 degrees and within the total end ROM offered by the design.

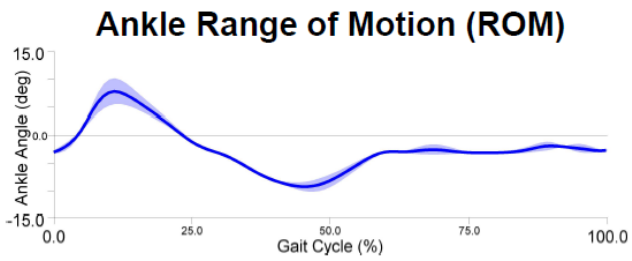

Figure 11. Mean ± 1 standard deviation ankle range-of-motion during normal walking speed.

7.0 DISCUSSION

To restore both effective walking mobility and stable standing balance, previous work suggests that ankle-foot prostheses should incorporate two distinct functional modes [5]. This paper describes the design evolution of a bimodal ankle-foot prosthesis that can accommodate both functional modes by locking the ankle when the user is standing (resulting in a flat effective rocker shape) and unlocking the ankle when the user is walking (resulting in a curved effective rocker shape). In an effort to address an additional customer requirement, which was to provide an ankle that can lock at a continuous range of angles (±12 degrees from neutral) to allow for standing on non-level surfaces, our group revised the design of a first-generation prototype to successfully incorporate a hydraulic locking mechanism. Three primary design specifications guided the development of this hydraulic locking mechanism, which to date, has been cycle tested to 1.2 million cycles. To accommodate the placement of the hydraulic cylinder within the ankle's design envelope, the configuration of elastomeric bumpers (influencing the rocker shape of the prosthesis during walking) was modified. Furthermore, the rigid footplate of the first-generation prototype was replaced by a rigid sidewall structure and flexible keel. To evaluate the extent to which this new design provided a biomimetic ROS during standing, swaying, and walking, motion analysis data were collected on a single lower-limb prosthesis user.

Human subject testing confirmed that when the bimodal ankle was locked, the amount of overlap between the rigid sidewall and flexible keel provided an extremely flat base of support, with a ROS radius much larger during swaying than that of walking (Fig 10). In fact, the ROS radius measured during swaying exceeded the target of twice the total leg length (typical for the anatomical ankle-foot system). When unlocked, the bimodal ankle conformed to a curved effective shape during walking, with a ROS radius only slightly larger than the target observed for the anatomical foot. Two factors likely explain this result: 1) the durometer of the anterior elastomeric bumper was

likely too stiff (supported by subjective feedback from the user) and 2) the subject was not wearing a foot shell or shoe during testing. Rather than revise the sidewall geometry to reduce the radius of curvature during walking, testing will be repeated with a softer anterior bumper and with the subject wearing a foot shell and shoe. Future work will also focus on the development of a theoretical model to guide bumper selection.

Encouraged by the biomimetic function of the hydraulic bimodal ankle-foot design, future testing with lower-limb prosthesis users is planned to explore the extent to which this design improves standing balance on both level and non-level surfaces. Balance outcomes (e.g., Sensory Organization Test, Limits of Stability Test, Duke Mobility Skills Profile, Four Stage Balance Test, and 2-Minute Walk Test) will be compared while subjects use the ankle in both the locked and unlocked modes. The capacity for an automatic switching algorithm, designed to appropriately detect and switch between modes as users transition between walking and standing tasks, will also be evaluated as subjects perform several common activities of daily living. These tests will evaluate the function of the device in more realistic use scenarios.

ACKNOWLEDGEMENTS

This work was supported by a grant to WillowWood from the Department of Health and Human Services Administration for Community Living, NIDILRR Small Business Innovation Research Grant No. 90BISB0010-01-00. This material is declared a work of the U.S. Government and is not subject to copyright protection in the United States. Approved for public release; distribution is unlimited.

REFERENCES

[1] Hansen, A., D. Childress, and E. Knox (2004). "Roll-over shapes of human locomotor systems: Effects of walking speed." *Clin Biomech (Bristol, Avon)* 19(4): 407-414.

[2] Hansen, A., and D. Childress (2005). "Effects of adding weight to the torso on roll-over characteristics of walking." *J Rehabil Res Dev* 42(3): 381-390.

[3] Hansen, A., and D. Childress (2004). "Effects of shoe heel height on biologic roll-over characteristics during walking." *J Rehabil Res Dev* 41(4): 547-554.

[4] Wang, C.C., and A.H. Hansen (2010). "Response of able-bodied persons to changes in shoe rocker radius during walking: Changes in ankle kinematics to maintain a consistent roll-over shape." *J Biomech* 43: 2288-2293.

[5] Hansen, A.H., and C.C. Wang (2010). "Effective rocker shapes used by able-bodied persons for walking and fore-aft swaying: Implication for design of ankle-foot prostheses." *Gait Posture* 32(2): 181-184.

[6] Koehler-McNicholas, S.R., B.C.S. Slater, K. Koester, E.A. Nickel, J.E. Ferguson, and A.H. Hansen (2018). "Bimodal ankle-foot prosthesis for enhanced standing stability." *PLoS one* 13(9): e0204512.

[7] Miller, W.C., A.B. Deathe, M. Speechley, and J. Koval (2001). "The influence of falling, fear of falling, and balance confidence on prosthetic mobility and social activity among individuals with a lower extremity amputation." *Arch Phys Med Rehabil* 82(9): 1238-1244.

[8] Miller, W.C., and A.B. Deathe (2011). "The influence of balance confidence on social activity after discharge from prosthetic rehabilitation for first lower limb amputation." *Prosthet Orthot Int* 35(4): 379-385.

[9] Asano, M., P. Rushton, W.C. Miller, and B.A. Deathe (2008). "Predictors of quality of life among individuals who have a lower limb amputation." *Prosthet Orthot Int* 32(2): 231-243.

[10] Hansen, A.H., and E.A. Nickel (2013). "Development of a bimodal ankle-foot prosthesis for walking and standing/swaying." *J Med Dev* 7(3): 035001.

[11] Hansen, A.H., M.R. Meier, M. Sam, D.S. Childress, and M.L. Edwards (2003). "Alignment of trans-tibial prostheses based on roll-over shape principles." *Prosthet Orthot Int* 27(2): 89-99.

